Radiation Measurements 143 (2021) 106580

Contents lists available at ScienceDirect

Radiation Measurements

journal homepage: http://www.elsevier.com/locate/radmeas

Investigation into the performance of dose rate measurement instruments used in non-governmental networks

Viacheslav Morosh [a,*], Annette Röttger [a], Stefan Neumaier [a], Faton Krasniqi [a], Miloš Živanović [b], Nikola Kržanović [b], Gordana Pantelić [b], Giorgia Iurlaro [c], Francesca Mariotti [c], Luciano Sperandio [c], Steven Bell [d], Sotiris Ioannidis [d], Martin Kelly [d], Marco Sangiorgi [e]

[a] Physikalisch-Technische Bundesanstalt (PTB), Bundesallee100, Braunschweig, 38116, Germany
[b] Vinca Institute of Nuclear Sciences (VINS), University of Belgrade, Serbia
[c] Italian National Agency for New Technologies, Energy and Sustainable Economic Development (ENEA), Italy
[d] National Physical Laboratory Management Limited (NPL), United Kingdom
[e] European Commission, Joint Research Centre (JRC), Ispra, Italy

ARTICLE INFO

Keywords:
Preparedness
Measurements of the ambient dose equivalent rate H*(10)
Radiation protection
Non-governmental dosimetry networks
Radiological accident or incident
Dose rate meter
Geiger tube detector

ABSTRACT

In the aftermath of a nuclear or radiological accident, an extended mapping of reliable dose rate values is of key importance for any governmental decision and countermeasures. Presently, numerous dosimetry network stations, operated by the national governments of the member states in Europe, provide such dose rate data on an hourly basis. Nevertheless, there are large areas in Europe that are not covered at all by these early warning networks and other areas that show only a low density of governmental network stations. Hence, there may be a significant lack of information in case of a nuclear or radiological emergency. As a consequence of the Fukushima Daiichi nuclear power plant accidents in 2011, a number of non-governmental radiation monitoring networks (NRMN) appeared on the internet, providing dose rate data based on stationary as well as on mobile measurements of ionizing radiation by laypersons. Especially the mobile detectors are able to cover large areas in short time. Therefore, it is of considerable importance to investigate the feasibility of using dose rate data from non-governmental networks as a complementary input to the European Radiological Data Exchange Platform (EURDEP). Within the European Metrology Program for Innovation and Research (EMPIR), the project 16ENV04 "Preparedness" has studied the metrological relevance of such non-governmental dose rate data (also called crowd-sourced radiological monitoring) in the most comprehensive way so far. Sixteen different dose rate detector systems (in general 4 of each type, plus 2 types with 2 detectors, i.e. 68 detectors in total) used in NRMN have been investigated for the reliability of their data and the corresponding networks, and their data provision to the public were analyzed. The most relevant performance parameters of dosimetry systems (detector's inherent background, energy dependence and linearity of the response as well as the response to secondary cosmic radiation, the sensitivity to small increases of the dose rate and finally the stability of the detector's indication at various climatic conditions - temperature and humidity) have been investigated for fourteen representative types of non-governmental dose rate measuring instruments. Results of this comprehensive performance study of the simple, light-weighted and cheap dose rate meters used in NRMN, and conclusions on the feasibility of using their data for governmental monitoring in case of a nuclear or radiological emergency are presented.

1. Introduction

As a consequence of the Chernobyl nuclear accident in 1986 and based on the Council Decision 87/600/Euratom, the European countries began to expand their radiological early warning networks. Today more than 5500 stations are in operation and provide data on an hourly basis to the European Radiological Data Exchange Platform (EURDEP) of the European Commission (EC) (Sangiorgi et al., 2020). EURDEP serves as the central automatic data management system for the radiological data of the early warning networks in Europe, operated by the EC Joint

* Corresponding author.
E-mail address: viacheslav.morosh@ptb.de (V. Morosh).

https://doi.org/10.1016/j.radmeas.2021.106580
Received 7 December 2020; Received in revised form 17 March 2021; Accepted 6 April 2021
Available online 12 April 2021

Research Center in Ispra (Italy). The radiological data from the national European networks, especially the comprehensive map of ambient dose rate values, collected by EURDEP are available to the EC Member States but also to the general public. This information and its reliability are of key importance for any official decision on countermeasures in case of a nuclear or radiological emergency.

After the nuclear accidents in Fukushima in 2011, various non-governmental radiation monitoring networks (NRMN) were established in the scope of citizen science projects organized by private persons or by manufacturers of dose rate meters. The measuring instruments used in the non-governmental networks (MINNs) are typically dose rate meters or counters based on Geiger Muller (GM) sensors. The networks operate as internet cloud servers that store data, either manually uploaded by their users or automatically transmitted by the MINNs. Finally, the dose rate data are visualized on a world map and published on web sites with open public access. The number of monitoring stations – in most cases equipped with commercially available, simple and cheap dose rate meters and run by private citizens worldwide at their homes or mobile (e.g. carried by private cars) - has continuously grown after the Fukushima accident. The persistent development of "Internet of Things" (IoT) technologies in combination with quick accessibility of the broad public to its achievements will presumably keep this trend going, especially in case of any upcoming nuclear or radiological event.

The European joint research project 16ENV04 "Mobile detection of ionizing radiation following a nuclear or radiological incident" (shortly named "Preparedness") (http://www.preparedness-e, 2020), (Neumaier et al., 2019), (V04 Preparedness and Publi, 2018), funded by the European Metrology Program for Innovation and Research (EMPIR), started in 2017 with a duration of three years. The project's main objectives are the development of reliable instrumentation and methods necessary in the field of radiation protection in the aftermath of a nuclear or radiological emergency to quickly provide quantitative data on the activity concentrations and dose rate levels in contaminated areas after a severe release of radioactivity. In this context, the work package "Monitoring of ionizing radiation by non-governmental networks" of the project raises the question whether non-governmental networks may support and complement official dose rate data, like those provided by EURDEP, and evaluates the reliability of such crowd-sourced dose rate data based on a metrological approach.

As a first step, a study of the currently existing non-governmental networks was performed (Iurlaro et al., 2018a), (Iurlaro et al., 2018b), (Sperandio et al., 2018), (Report 92 - Radiatio, 2015). Then the project partners PTB, NPL, ENEA and VINS selected representative MINNs that are currently available on the market to investigate the reliability of their dose rate data in terms of the ambient dose equivalent rate $\dot{H}^{*}(10)$ using the metrological facilities of the national metrology institutes and the designated institutions involved in the project.

Finally, the partners tested 18 different MINN types under calibration laboratory conditions. The complete study intended to test the linearity and energy dependence of the response at the home facilities of the participating institutions. The remaining tests took place at PTB reference facilities in Brunswick (Germany) and were organized as an intercomparison campaign in June 2019, comprising all MINNs in the project. The intercomparison covered measurements of inherent background, response to secondary cosmic radiation (SCR), climatic test (influence of variation in air temperature and humidity) and detection of small dose rate changes caused by artificial gamma ray photon sources in the natural environment.

This paper summarizes and discusses the various results of the most comprehensive and systematic study of the performance of MINNs.

1.1. Non-governmental networks

Civil usage of nuclear energy in power plants may pose, in case of accidents or serious incidents, a radiological risk to the population. In some countries, public concern has made authorities object to nuclear power completely (e. g. Denmark, Italy, Austria and Germany). This refusal process was first ignited by the catastrophic accident of Chernobyl and later by the one of Fukushima, both resulting in a largely contaminated area where it will be dangerous to live in for decades due to the high levels of radiation caused by the relatively long half-life (e. g. 30 years for Cs-137) of the radionuclides in the fallout. In other countries, a strong public interest in this subject can be perceived by the development of independent or non-governmental monitoring networks of radiation in the scope of citizen science. Residents of Japan, for example, have purchased thousands of dosimeters for their personal use and non-governmental organizations - for the first time in history - have begun taking measurements following the release of radionuclides and share these data with others (Report 92 - Radiatio, 2015).

However, the nuclear power plants are not the only source of possible radioactive contaminations. Atomic weapon testing, medical, industrial and military use of ionizing radiation, nuclear waste storages, "dirty bombs" in the hands of terrorists, secondary exposure through contaminated persons are all examples for the release or distribution of radioactive material in the environment while contaminating an area, the food or drinking water supplies and threatening the safety of the population. The worldwide expansion of NRMNs may contribute substantially to the safety precautions in case of radiological accidents serving as an additional source of information for decision makers, depending on the quality of these data.

In the framework of the project 16ENV04 "Preparedness" a survey of currently existing global NRMNs has been conducted and the results can be found in (Iurlaro et al., 2018a), (Iurlaro et al., 2018b), (Sperandio et al., 2018). Additional general aspects regarding data provision, MINN operations and data safety in the NRMNs will be discussed in the following.

One such aspect is the spatial limitation of the provided data. A measurement by a fixed monitoring station in the NRMN provides only information on dose rates at its local position with receptivity of a few meters around it and hundreds of km between the stations. Moreover, the horizontal distribution of the radioactive fallout can depend on the local ground topography and weather conditions. Rain, wind and hillslopes can create inhomogeneities in the distribution of radioactive contaminations (Wallbrink and Murray, 1993), (Komissarov and Ogura, 2017), (Chartin et al., 2017). This dynamic process can lead to a redistribution or migration of the initial fallout depending on the type of the initial deposition (wet or dry) (Basuki et al., 2020), (Bonnett, 1990), soil properties (Poreba et al., 2003), vegetation (Bunzl et al., 1989), (Livens et al., 1992) and land use (Gonze and Calmon, 2017), (Yoshimura et al., 2016).

Another aspect is the lack of data protection from being faked. False data can be produced in two ways depending on the kind of data transmission to the server. If manually uploaded to the network server, the operator of the station has unlimited access to the measured data. The protocol files have either simple txt, csv or xlsx (MS Excel) format and can easily be edited or created. MINNs which send the data automatically can be manipulated to generate high dose rate data by placing a gamma source close to it.

Finally, the origin and independence of the NRMN data is not always clear. Some NRMN argue for using input data verification mechanisms that prevent the upload of malicious data (Brown et al., 2016). The network operators are best positioned to verify uploaded data, but even in this case it is the individual who decides what data will be made public on the map.

Some efforts have been made to calibrate and validate indications of the instruments used in the SAFECAST network (Coletti et al., 2017), (Hultquist and Cervone, 2018), but most of the currently existing NRMNs have no descriptions or recommendations of the exact measurement procedure. Unfortunately, the operators have no possibility of specifying the procedure they use to carry out the measurements or to

describe peculiarities (buildings, forest, water etc.) of the location. However, the knowledge of the height and orientation of the detector and information about the environment can be very helpful for data interpretation or analysis.

Surely, the current state is only a snapshot of the development of the NRMNs as a branch of IoT and citizen science. Safety issues, comparability and reliability of the delivered information are important aspects of this development and will ensure the use of this instrument for critical official decisions.

1.2. Instruments used in non-governmental networks

The main active users of NRMNs are civilians who are in possession of relatively simple counters, dose or dose rate meters available at internet shops. The devices in this study are equipped with different Geiger-Müller (GM) sensor types. Relatively simple built-in electronics ensures the operation and reading of the sensor and the processing of the counting statistics. The GM tubes are not energy compensated in any of the investigated MINN types. Plastic or aluminum serves as housing material for the MINNs with some of them do not even have a housing. The calculation of the dose rate is mostly done by multiplication of the count rate by a conversion factor without details about the origin of its value. Finally, the MINN types and the used GM sensors, whose properties have been investigated in this study, are listed in Table 1.

The different MINN types are anonymized by assigning random numbers (in a set of 1–18) to each MINN type which are consistent in all results throughout this work. Each MINN type is represented by four (1–9, 11–16 and 18) or two (10 and 17) individual dose rate meters with equivalent electronic components.

The GM sensor is the essential part of a dose rate meter whose behavior dominantly defines the main MINN characteristics. For comparison purpose, five categories of installed GM tubes with distinctive constructive traits were defined. As such, the shape and material of the GM tube walls, gas mixture and the number of sensors were selected:

Stainless steel and glass are the materials often utilized as GM tube walls. “Short” and “long” describe the tube’s shape with the lengths in the range of 2.5 cm–3.5 cm and 7 cm to 10.5 cm, respectively. Their diameters are comparable. “Pancake” has a cylindrical shape with the diameter much larger than the height. Category V is divided into two subcategories: a) a combination of two GM tubes with identical length and metal walls; b) a combination of a long and a short GM tube with glass capsules. These categorizations will allow us to analyze the test results with the knowledge of the constructive characteristics of the GM tubes used.

In this work, the focus will be on the MINN’s performance in gamma and X-ray photon fields. Thus, the presence of an entry window in some GM tubes intended for the detection of alpha and beta radiation is of less importance. Moreover, devices with selectable measurement modes are set up for the detection of gamma radiation only. Note, that in this mode the measurement of dose rate in some X-ray fields is also possible.

At the time of the publication the tests of the response to changes of the ambient climatic conditions for the MINN types 5, 6, 11, 15 have not been completed due to organizational issues (limited access to the working place and to the testing facilities) in combination with the worldwide pandemic COVID-19 situation. Those results and the results of the environmental tests, which have been conducted in June 2019 in the framework of the MINN intercomparison at PTB facilities, for the MINN type 6 will be published elsewhere.

Table 1
The MINN types and GM sensors selected for testing in the framework of the EMPIR project “Preparedness”.

MINN type	GM tube type
Gamma Scout	LND 712
Rad 100	LND 712
RadAlert Monitor 200	LND 712
Monitor 4 KIT	LND 712
µRAD Monitor A3	SI-29 BG
GMC 500+:	SI-29 BG and M 4011
Mazur PRM-7000	LND 713
uRAD Monitor A3.4	SBM 20
MyGeiger ver.3 pro	SBM 20
uRAD Monitor KIT1	SBM 20
Radex RD 1212 BT	SBM 20
Soeks Quantum	2 x SBM 20-1
Radex RD1706	2 x SBM 20-1
Radex RD1503+	SBM 20-1
GMC300E+	M 4011
GMC320+	M 4011
bGeigie Nano	LND 7317
Inspector Alert V2	LND 7317

Table 2
GM tube categories of the investigated MINNs.

Category	I	II	III	IV	V
Description	short tube, metal casing, gas mixture: neon, halogen	long tube, metal casing, gas mixture: neon, argon, halogen	long tube, glass casing	pancake shaped tube, metal casing, gas mixture: neon, halogen	combination of two a) equal, b) different categories of tubes
MINN type	1, 2, 3, 4, 5, 6	7, 8, 9, 10, 11	12, 13	14, 15	a) 16, 17 b) 18

2. Experimental details and results

2.1. General

The reading of a MINN $\dot{G}_{MINN}$ is made up of several components which can be differently pronounced depending on the physical properties of the detector system (materials and electronics) and on the radiation field (energy, dose rate) (Wissmann, 2006), (Bossew et al., 2017):

$$\dot{G}_{MINN} = \dot{M} + q_{terr}\cdot\dot{H}^{*}(10)_{ref,\ terr} + q_{SCR}\cdot\dot{H}^{*}(10)_{ref,\ SCR} + q_{art}\cdot\dot{H}^{*}(10)_{ref,\ art} \quad (1)$$

where q characterizes the sensitivity of the MINN to a photon field. $\dot{H}^{*}(10)_{ref,\ terr}$, $\dot{H}^{*}(10)_{ref,\ SCR}$ and $\dot{H}^{*}(10)_{ref,\ art}$ are the reference ambient dose equivalent rates arising from radiation fields of terrestrial, secondary cosmic or artificial origin, respectively. The sensitivity of a detector can be considered as nearly constant for the contributions originating from the natural radiation sources at a fixed location whereas the factor q_{art} can strongly vary with energy and dose rate of the artificial radiation coming from “outside” depending on the source quality. This is due to the energy dependence of the interaction probability of the incident photons with the sensor and relatively long recovery periods from complete ionization in the sensor interior, i.e. long dead times. Moreover, MINN housings and sensor walls impose a critical reduction of the q_{art} factor in the very low (<30 keV) photon energy region. Thus, the knowledge of the photon field properties might be essential for proper measurement of the ambient dose equivalent rate $\dot{H}^{*}(10)$ when using MINNs with uncompensated GM sensor types. $\dot{M}$ represents the MINN reading in absence of any type of ionizing radiation, also referred to as inherent background or self-effect of the measurement instrument. In case of GM tubes where high voltage is applied to the gas volume, this effect is likely caused by spontaneous discharges due to a dielectric breakdown.

2.2. Uncertainties

In this study, the uncertainties were evaluated in accordance with the recommendations by GUM (International Organization for Standardization, 1995). Reference values served as a verification of the MINN measurement results. For inherent background, linearity and energy dependence tests, the traceable reference values including their uncertainties were provided by the facilities. At plume simulation and sensitivity to SCR tests the reference instruments calibrated and traceable to PTB primary standard were employed. Both MINN and reference results were obtained as the mean values of the repeated readout from the corresponding instrument, respectively. The acquisition times - the time interval for regular storage of the counter or dose rate meter values during permanent operation of the instrument-for MINNs and for the reference instruments were set to 1 min when possible.

Readings from MINNs and from reference instruments were averaged within one continuous period of irradiation and the experimental standard deviation of the mean was calculated according to type A evaluation described in (International Organization for Standardization, 1995). In case when the subtraction of (inherent) background or a subsequent calculation (e. g. relative response) was performed the combined standard uncertainty for uncorrelated input quantities was calculated.

For the representation of results by type, all mean values per MINN type were averaged. The type-related uncertainty was defined as the maximum of type An uncertainties assigned to the MINNs of the same type. The exception to this rule is the climatic test where only one MINN of each type participated. Consequently, the MINN type uncertainty was equated to the uncertainty of this MINN.

All results are finally reported with expanded uncertainties with the coverage factor $k = 2$ or 95% level of confidence.

2.3. Measurements of MINN's inherent background

2.3.1. General

For the determination of the inherent background of the MINNs, a location with very low background radiation level is required. One of the PTB's facilities (UDO II), established in a salt mine at a depth of about 430 m underground, offers the testing environment with a constant background radiation as low as $\dot{H}^*(10)_{UDOII,\ BG} = (1.4 \pm 0.2)$ nSv h^{-1} (Neumaier and Dombrowski, 2014), (Röttger and Kessler, 2019). This very low background radiation level mainly results from K-40 in the rock salt and a small contribution from the small amount of progeny of radon gas in air. The secondary cosmic radiation is reduced by more than 4 orders of magnitude and hence negligible (Neumaier et al., 2000a). Using a "lead castle" construction inside the lab allows a further reduction of the background radiation level to only $\dot{H}^*(10)_{UDOII,\ "lead\ castle"} \approx 0.1$ nSv h^{-1}. A preliminary test showed no difference between the measurements of the inherent background of some selected MINNs surrounded by or without the "lead castle" construction. Consequently, the inherent background of all MINNs was determined by placing them on the tables in the underground laboratory room.

Under these conditions, the MINNs are expected to display values related to their own noise of the installed GM tube, electronic components and built-in computation algorithm. Equation (1) has here the form:

$$\dot{G}_{MINN} = \dot{M}. \tag{2}$$

Moreover, the underground lab provides a photon calibration facility with various gamma sources (Am-241, Cs-137, Co-57, Co-60, sealed Ra-226 in equilibrium with its progeny) which can be used to generate collimated photon fields with ambient dose equivalent rate values of a few tens up to a few hundreds of nSv h^{-1} traceable to PTB primary standards.

2.3.2. Results

The MINNs were subjected to an environment with extremely low radiation level at UDOII for about 4 h. This time period results in a relative uncertainty of about 7% which arises from counting statistics for the smallest observed averaged MINN reading of 1 cpm (1 count per minute). The reference value (solid line) of the facility background $\dot{H}^*(10)_{BG,\ UDOII}$ has been subtracted from the mean values of the MINN readings. The results of these measurements are shown in the plot of Fig. 1.

One finds that in most cases the measured inherent background for individual MINNs corresponds with the average inherent background of the MINN type (within measurement uncertainty) with the exception of the types 2 and 13, where one value is significantly different from the other three, and the type 3 where two values are significantly different. Due to the small size of the sample (only 4 MINNs of the same type), it is not possible to know whether this deviation was typical for the type or caused by possible variations in the characteristics of the electronic parts (sensor, high voltage or readout electronics) or a device failure. However, the MINN type mean value calculated using all MINNs representing the type will be applied for calculations throughout this work.

The MINN type mean values demonstrate a significant scatter of the investigated parameter, however, there is always a clear elevation of the MINN self-effect over $\dot{H}^*(10)_{UDOII,\ BG}$. The possible causes can be either a considerable variation in the GM sensor's own noise or instability of the electronics or the kind of data processing implemented in the MINN, e.g. subtraction from the measured quantity (cps, cpm or $\dot{H}^*(10)$) of a constant value attributed to an inherent background.

By means of the categories defined in Table 2, one finds that the MINN types 1- 6with the small GM tubes (category I) show the lowest inherent background values. In contrast, the types 7, 8, 10, 11, 12, and 13 with GM tubes of the categories II and III almost all demonstrate a similar increase of the inherent background values except for the type 9. The outstandingly large self-effect of the type 9 could be explained by less stable electronics for high voltage supply or by the type of data processing. The MINN types with the sensor of category IV have a comparably larger volume of GM tubes and demonstrate low self-effect, instead. Surprisingly, the MINN types of the category V a) and b) have their inherent backgrounds comparable with those of category II; even though their GM sensors are of the same type, however differing in the number. The MINN types 10 and 17 were represented only by two units. They lack an automatic data acquisition and have been read out by the eye in a 10-min tact. The comparably smaller data samples from both dose rate meters representing the types have been combined for calculation of the error bars which are applied to both MINNs of one type. The observed variations of the inherent background values might be the result of a specific on-board data processing which subtracts a value attributed to this characteristic from each measurement, or of the differences in the quality of the GM tubes or the stability of their operation.

In addition to the long-term exposure to the low background radiation of UDO II described above, four MINNs of different types have been randomly picked out for irradiation using collimated Cs-137 gamma ray sources with different activities in the UDOII laboratory. The MINNs belonged to the types 1, 7, 14 and 16 and can be considered as representative for all types in this study because they cover 4 different categories. The irradiation results were used to perform linear regression that is shown in the plots of Fig. 2. The laboratory background $\dot{H}^*(10)_{BG,\ UDOII}$ was subtracted from the mean values.

In Table 3 the results for the inherent background values of the four MINN types, derived either from long-time measurements or from the linear regression of irradiation data both carried out in PTB's UDOII laboratory, are summarized. For all 4 MINN types both results agree within the measurement uncertainty. For calculations throughout this paper the inherent background values determined by long-term measurements at UDOII will be preferred due to smaller uncertainties for all

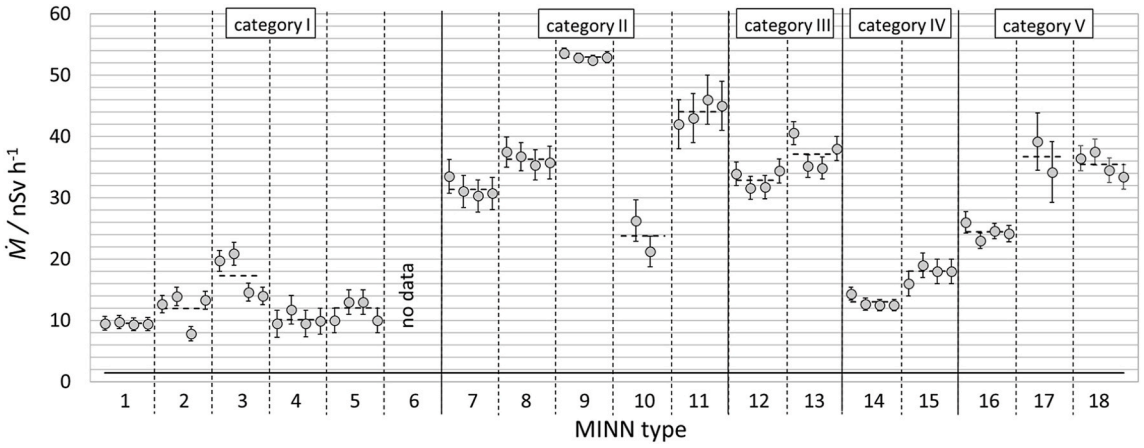

Fig. 1. Inherent background of individual MINNs (points), measured in the PTB underground laboratory UDO II. The dashed horizontal lines depict the MINN type mean values, the solid horizontal line shows the laboratory background level of 1.4 nSvh^{-1}and the solid vertical lines show categories after Table 2.

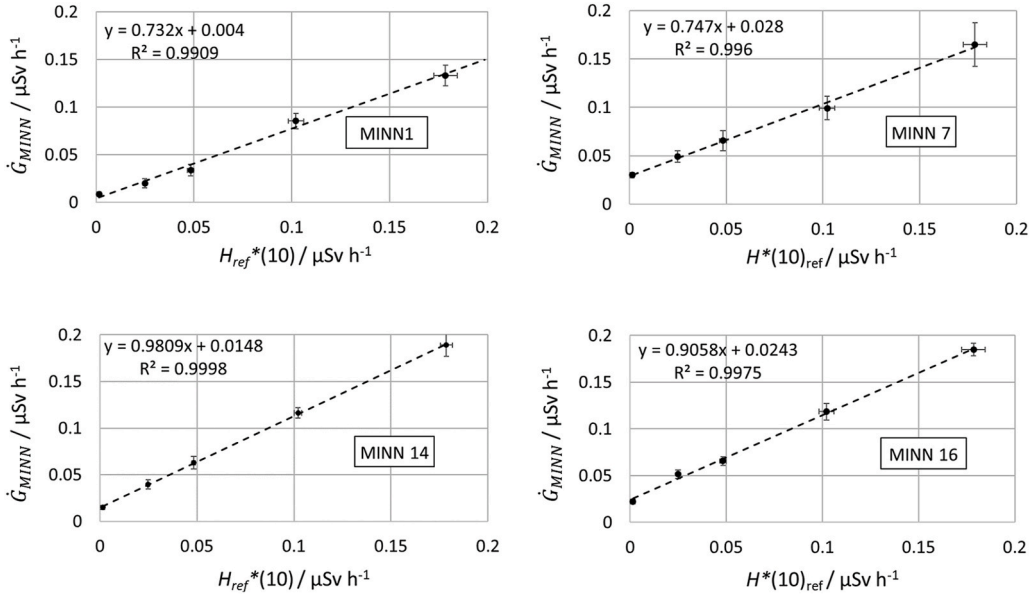

Fig. 2. Linear regression for four MINNs irradiated in UDOII laboratory.

Table 3
Inherent background evaluated from linear regression for the four MINNs irradiated in UDOII laboratory and comparison with the values received from long-term measurements.

MINN	Long-term exposure, µSv/h	Linear regression, µSv/h
1	0.0081 ± 0.0012	0.004 ± 0.008
7	0.0303 ± 0.0026	0.028 ± 0.005
14	0.0144 ± 0.0012	0.015 ± 0.002
16	0.0242 ± 0.0014	0.024 ± 0.005

MINN types.

2.4. Secondary cosmic radiation (SCR) measurements

2.4.1. General

An Environment with negligibly low levels of terrestrial and artificial radiation was selected for the determination of the MINN's response to the SCR. Therefore, the measurements were conducted using the PTB floating platform on a lake near Brunswick (Germany). The platform is made of low Z materials and is positioned at least 100 m from the shore. The water's depth is about 3 m which provides an adequate shielding from terrestrial radiation. A negligible portion of the terrestrial component (about 1 nSv h^{-1} (Saez Vergara et al., 2007)) can still reach the platform through the scatterings in the air. The reference value for the ambient dose equivalent rate of the SCR on ground, $\dot{H}^{*}(10)_{SCR} = (29 \pm 4)$ nSv h^{-1} is measured using detectors - MUDOS: Muon Dosimetry System (Wissmann et al., 2005) - which are installed on the reference site for environmental dosimetry on PTB's premises. and which are sensitive to the charged components of the SCR, such as muons and electrons. A detailed description of these instruments can be found in (Wissmann et al., 2005) and (Neumaier and Dombrowski, 2014).

During the measurement of the SCR sensitivity, MINNs were spread on a platform on top of some large plastic trunks. In many cases the reference orientation of the MINNs is not specified by the manufacturers. Moreover, in practical use the orientation of the MINNs might be arbitrary. A test conducted earlier showed no statistically significant difference between the vertical and horizontal MINN orientations for measurements of the SCR sensitivity. Therefore, for the current study the MINNs were laid out with their front panel (display side) upwards. Positioned in such manner, the longer dimensions of GM tubes have

been subjected to the incident direction of the particles making up the SCR. MINNs with the pancake-shaped sensors were placed with the tube's window facing downwards so that the display is then turned to the observer.

In order to avoid a contribution of the radiation originating from human bodies, measurements started only after all participants were transported back to the lakeshore. The MINNs were exposed to the SCR for 1.5 h.

Equation (1) can be rewritten for this test as follows:

$$\dot{G}_{MINN} = \dot{M} + q_{SCR} \cdot \dot{H}^{*}(10)_{ref,\ SCR}. \quad (3)$$

2.4.2. Results

The results of this test are depicted in Fig. 3. The inherent background of each individual MINN determined in the previous section has been subtracted.

The MINNs demonstrate the expected behavior of detectors using gas-filled sensors (Neumaier and Dombrowski, 2014), (Wissmann et al., 2005), (Dombrowski et al., 2009). Almost all types have significant overresponse for the SCR which mainly consists of particles with high energies. Only one type was able to reproduce the reference value of the SCR within experimental uncertainty. Remarkably, this MINN type 9 has the highest inherent background of all types in this work.

2.5. Response to different ambient conditions

The employment of the MINNs under different ambient conditions at the measurement location requires the readings to be insensitive to temperature and humidity changes. This test was carried out at PTB using the climatic cabinet which has the control routine for calibrated temperature t and relative humidity rH adjustment. Additionally, the investigated dose rate meters were irradiated during the whole test period using a Cs-137 gamma source to generate indication in the order of a few μSv h^{-1} to reduce statistical uncertainty. The temperature range specified by the manufacturers was found to be between −20 °C and +50 °C (max. +60 °C). If this was not specified, stable operation was expected up to at least +50 °C – the temperature that can be reached inside a car (even outside in some places) in summer. The relative humidity values were chosen in the range between 50% and 95% (non-condensing).

The test routine consisted of five periods of static ambient conditions with continuous changes in between. Each of the conditions was maintained for about 4 h, however, only the last hour data was taken for the analysis. This was necessary because normally there is a lag in the thermalization of the MINN's interior and the GM's sensor. The first and the last periods were referred to as normal conditions (20 °C, 65% rH). The MINN's mean readings at normal conditions $\dot{G}_{n.c.}$ at the beginning of the test were used for the validation of the constant configuration of the experimental setup during the whole test, e. g. relative position of the source and the MINN which can likely be changed by vibrations of the climatic cabinet. The results in Fig. 4 are represented as the mean values of the MINN's indication $\dot{G}_{t,\ rH}$ calculated for a period with nominally constant t and rH, normalized by the mean value of the indication $\dot{G}_{n.c.}$ during the first period of the normal conditions.

The plot shows groups of bars corresponding to constant test conditions. Three different MINN types of the same manufacturer had problems to operate properly at the high temperature of 50 °C and 50% rH. During their continued operation all the logged results showed 0 cpm. After the temperature was reduced to 30 °C, the instruments

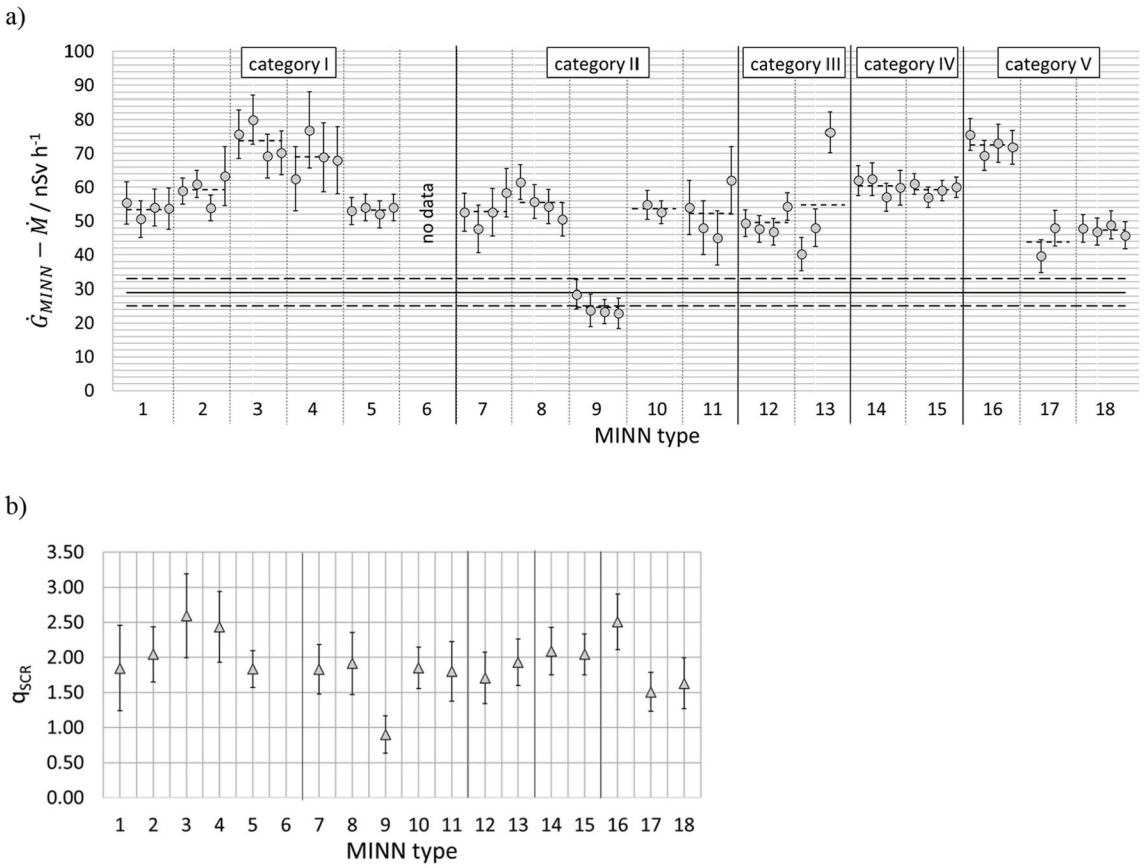

Fig. 3. a) Mean values of the indication during measurements on the lake platform in comparison with the reference value provided by detectors - MUDOS: Muon Dosimetry System (Wissmann et al., 2005) - operated on PTB reference site (long solid line). Long dash lines indicate the uncertainty of the reference value. Short dash lines show average values calculated for the MINN types; b) SCR sensitivity factors q_{SCR} of the investigated MINN types calculated with Eq. (1).

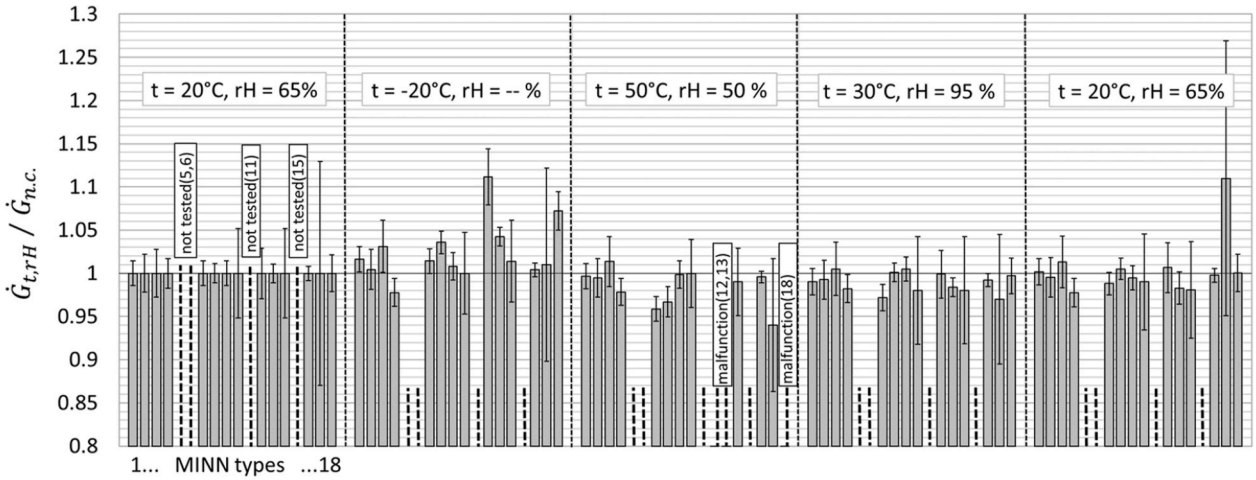

Fig. 4. Result of the climatic test carried out for one device of each MINN type. Three MINN types (12, 13 and 18) measured no radiation at a climatic condition and are labeled as "malfunction". Short vertical dashed lines indicate the MINN types which have not participated in the climatic test.

continued to operate normally. All remaining MINN types show stable behavior of the response in the investigated temperature and humidity range. At positive temperatures, independent of the humidity values, the mean indication of the majority of MINNs coincides with the mean value at normal conditions which corresponds to the relative response of the unity.

In terms of the IEC 60846–1 (International Electrotechnical Commission, 2009) standard, the deviation of the indication of a dose rate meter in the temperature range between −10 °C and 40 °C should not exceed −13% and +18%. In the relative humidity range of up to 85% at 35 °C, the maximum deviations between −9% and 11% should be satisfied. These requirements are fulfilled by all tested and working MINN types.

2.6. Linearity of the response

2.6.1. General

The response of a GM sensor is known to have linearity only in a limited range of dose rates, mainly due to the dead time effect (Corson and Wilson, 1962). In this study, we investigate this characteristic on MINNs, applying the procedure described below.

The MINNs were exposed one by one to the collimated gamma fields (Cs-137 or Co-60) in the gamma irradiation laboratories of the partner institutions in accordance with ISO 4037-1 standard (ISO 4037–1:2019, 2019). The ambient dose equivalent rate range was chosen to encompass values between 200 nSv h^{-1} and 900 μSv h^{-1}. In Germany, the reference levels for official intervention (according to the source www.bfs.de, last access November 2020) are defined as the effective doses of 10 mSv ("Sheltering") and 100 mSv ("Evacuation") of the external exposure in 7 days. These values approximately correspond to the $\dot{H}^*(10)$ values of 60 μSv h^{-1} and 600 μSv h^{-1} and are well covered by the selected interval.

The MINNs and the incident photon field were separated by a PMMA plate to establish the secondary charged particles equilibrium. The plate was placed close to the test device on the side of the incident photon flow. The reference point on the MINN housing and the orientation were chosen in accordance with the manufacturer's specifications. When that data was missing, reference orientation was anticipated from its shape and presence of the entry window. If the MINN had a window, it was directed to the incident photons, otherwise the rear panel of the MINN pointed towards the source so that the display would be turned to the observer. If the MINN had a selectable shielding, it was set for measurements of the gamma radiation. The duration of the irradiation and the acquisition time were selected by each laboratory and for each MINN type in such a way as to provide satisfactory statistics– resulting in standard deviation around 5% of the mean value or smaller - (e.g., if the acquisition time was 1 min, the irradiation time was at least 20 min, providing at least 18 measurement points or at least 400 counts at each constant ambient dose equivalent rate). Some measurement points coincided with the periods of the rise and fall of the ambient dose equivalent rate. These points were discarded from the calculations.

The analysis of the results was carried out from the point of view of the IEC 60846-1 standard. Criteria for dosimeters that have to be fulfilled to pass the formal procedure for certification as the ambient dose equivalent rate meter are in particular to be found in this document.

The relative response r is defined there as the quotient of the response $R = \frac{\dot{G}}{\dot{H}}$ with $\dot{G}$ the indicated MINN value, $\dot{H} = \dot{H}^*(10)_{Ref}$ the reference ambient dose equivalent rate in the adjusted field and the reference response $R_0 = \frac{\dot{G}_{r,0}}{\dot{H}_{r,0}}$ with $\dot{G}_{r,0}$ the indicated MINN value at some fixed conditions and $\dot{H}^*_{r,0}$ the corresponding reference value:

$$r = \frac{R}{R_0}. \tag{4}$$

This quantity allows us to eliminate possible inaccuracies of the calibration due to inappropriate procedure or variations in characteristics of the components (electronics or sensor) the instrument is made of.

The ambient dose equivalent rate $\dot{H}^*(10)_{r,0} = 10$ μSv h^{-1} of Cs-137 quality at the location of the MINN was defined as reference value for the linearity test.

2.6.2. Results

The 1-min values measured by a dose rate meter over the period of a single irradiation were averaged and the background was subtracted. The combined uncertainty of the mean was calculated. In the next step, the mean values of the four MINNs of the same type were averaged to represent the mean value of the MINN type. The maximum combined uncertainty of the four MINNs of the same type was used as the uncertainty for the type mean value and, consequently, for the calculation of the expanded uncertainty of the relative response with the coverage factor of two. The relative response was calculated using Eq. (4). The results of r for each MINN type are depicted in the plots of Fig. 5.

In the IEC 60846-1 document, the allowed deviations of the upper and the lower limits of the relative response are set between 22% and −15% (dashed lines), respectively. The MINN types 3–5, 10–15, 17, 18 satisfy completely the linearity limits in the tested dose rate range. In contrast, the MINN types 2, 7, 8, 16 cross the lower limit of the tolerable

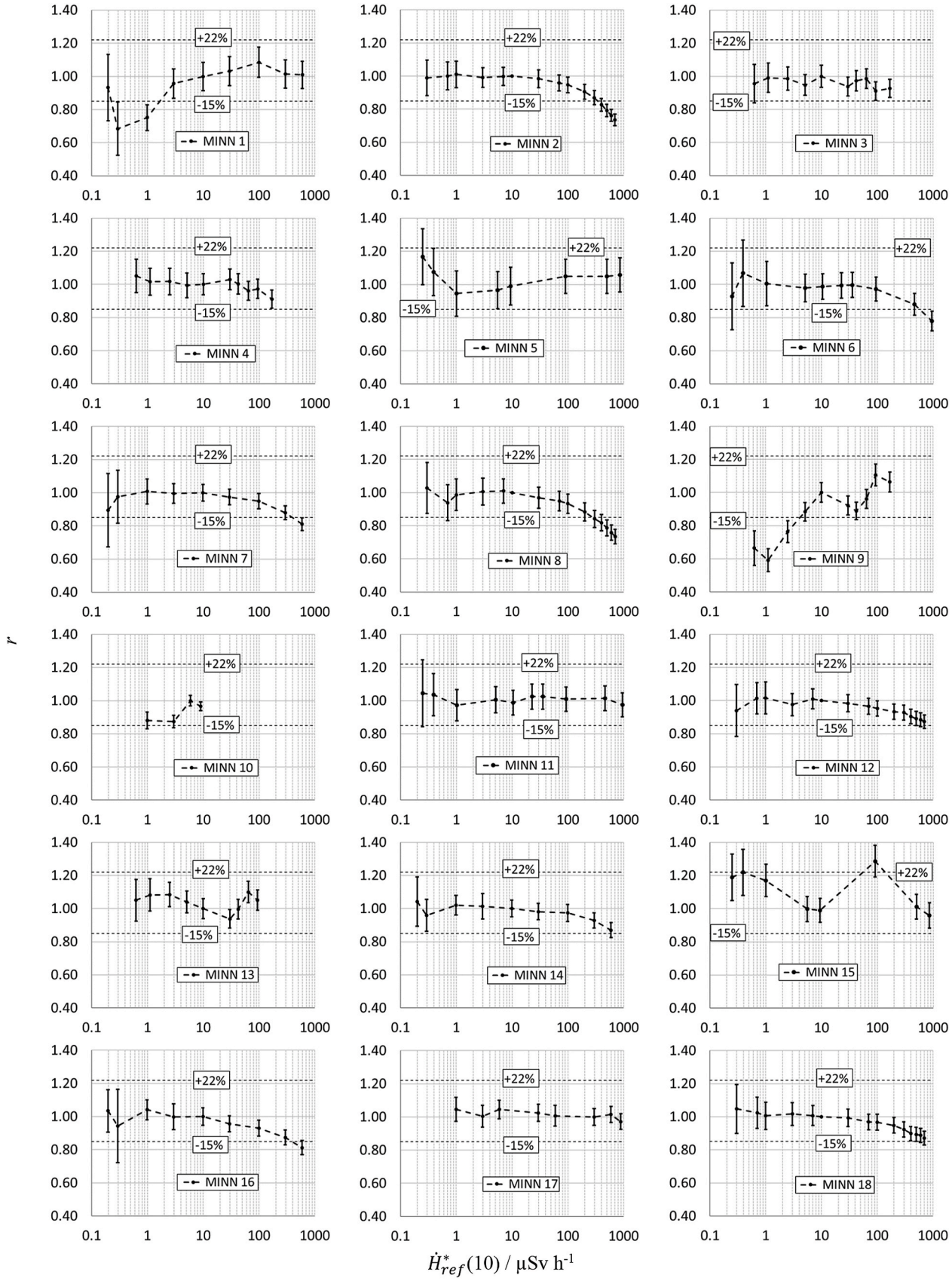

Fig. 5. Relative response of the tested MINN types. Dotted lines depict the upper and lower limits of maximum tolerable deviations of the relative response according to IEC 60846–1.

linearity region at around 500 μSv·h^{-1} and the MINN type 6 around 850 μSv·h^{-1}. Other exceptions are the types 1 and 9, where r falls below the lower limit but still satisfies the limits around 200 μSv·h^{-1} (MINN 1) and in the region beginning with 2 μSv·h^{-1} (MINN 1) or 3 μSv·h^{-1} (MINN 9) upwards. The MINN types 10 and 17 have factory-set limited dose rate range (as presented) and have been tested to read zero when operated out of this range.

2.7. Energy response

2.7.1. General

This test was conducted using the radiation qualities established according to ISO 4037–1 in the laboratories of the participating partner institutions. In accordance with IEC 60846, for covering the lower energy region, the N-Series qualities or Am-241 (MINN types 5, 6, 11, 15) were used. For higher energies the collimated photon beams of the nuclides Cs-137 and Co-60 have been applied. The ambient dose equivalent rate $\dot{H}^*(10)_{Ref,0}$ was maintained at constant value in the range of 10 μSv·h^{-1}–100 μSv·h^{-1}. The measurement procedure, the positioning of the MINNs and the evaluation of the results were the same as applied in the linearity test. The Cs-137 served as the reference quality.

2.7.2. Results

The data for the final representation was processed by the methods described above. In the diagram in Fig. 6 the results from the energy response for MINN types are shown.

For MINN types 5 and 15 the manufacturer recommended readout system was used. In this configuration it introduced additional dead time which limited measured number of counts, effectively. This effect is expected to be more significant when measurements were conducted in Am-241 field.

All the tested MINNs failed the requirements set by IEC 60846-1 by a high margin. The behavior of the MINN types is expected as they utilize energy uncompensated GM sensors whose efficiency is highly dependent on the energy of the incident photons (von Droste, 1937), (YukawaSakata, 1937). The relative response increased up to 11 times (MINN 9) at low energies between a few tens of keV up to about 120 keV.

2.8. Small dose rate changes on top of the natural background radiation (plume simulation)

2.8.1. General

The MINNs are used for measurements of dose rates produced by natural and artificial gamma photon sources. An important feature of the radiation fields in the environment is their dispersity and the presence of a large amount of Compton photons with different energies, i. e. scattered from the ground, plants, buildings and in the air. In contrast, gamma fields produced in laboratories are collimated and have a well-defined direction of incidence and less scattered components. A plume simulation test was carried out at PTB to investigate the behavior of the MINN types participating in this study under controlled radiological conditions in the natural environment close to a real-case scenario – flying by of radioactive clouds.

The location for this test was a meadow on PTB property near the neutron dosimetry laboratory building with a proton accelerator and a cyclotron inside. The time period for the plume simulation was chosen to coincide with the maintenance of the mentioned facilities to avoid their impact on the measurements.

The plume simulation setup (Fig. 7 a) was established to emulate the passing of a radioactive plume across the site. The employed in-house developed machine can incorporate up to four individual point-like gamma sources. It is equipped with different types of shielding used for the generation of constant radiation fields which, for dosimetry purposes, can be characterized by well-defined dose equivalent rates $\dot{H}^*(10)$ at a fixed distance. The sources are confined inside a lead box where they are "inactive", i.e. no radiation comes out. The source can automatically be moved from the lead box to one of the three vertically arranged positions where it is surrounded by material with "strong", "weak" and "no" shielding ability. The machine is usually put in place so that the gamma source has the central position relative to the test devices which are arranged along the circumference of the circle with 5 m radius.

During the plume simulation, three different point-like sources (Cs-137, Co-60, Ra-226) at the three different shielding positions were used to generate six dose equivalent rates. The Ra-226 source was put manually on top of the plume machine where sources are usually used without shielding. At that time, no other source was exposed.

A secondary standard Reuter Stokes ionization chamber (type RS-131) was installed in the circle as reference instrument and operated during the test to provide reference $\dot{H}^*(10)_{ref,\,art}$ values. It has been calibrated in the PTB underground laboratory UDOII with the reference values traceable to the primary standard.

At the beginning of the test, the level of the background dose rate was measured for at least 30 min. This was followed by six 30-min periods of irradiation with photon fields defined by the combination of the source and the shielding type. At the end, the background was measured again. The reference values of the dose equivalent rate of the gamma photon fields during the plume simulation test including their $k = 2$ confidence intervals are summarized in Table 4. The time periods were taken from the protocol of the plume machine, logged automatically by the control software.

In order to ensure that all MINNs have equal test conditions, a special fixation has been designed, constructed and provided for all participants. It consists of eight wooden boards with a length of 2.50 m, fixed on two height adjustable tripods distributed along the circle. All MINNs are attached to the boards using wooden holders. The radially adjustable holders allow shifting the MINNs along the radius to precisely define their position relative to the source. The MINNs are positioned in such a way that the geometrical middle of their Geiger tubes is about 1 m above the ground and 5 m to the source with 20 cm gaps in between. Additionally, vertical or horizontal orientation of the MINN was possible. For some of the types (1, 7, 14, 16) both positions were tested with no significant difference.

During the whole test, all MINNs are permanently running and storing data in defined time intervals. It was arranged among the participants to set 1 min as the data acquisition time. For some devices it was not possible to change this setting - for MINN 9 the acquisition time was 5 min.

For calculations in this section, Eq. (1) can be rewritten as:

$$\dot{G}_{MINN} = \dot{G}_{BG} + q_{art}\cdot\dot{H}^*(10)_{ref,\,art} \tag{5}$$

with $\dot{G}_{BG} = \dot{M} + q_{terr}\cdot\dot{H}^*(10)_{ref,\,terr} + q_{SCR}\cdot\dot{H}^*(10)_{ref,\,SCR}$ the averaged MINN indication during the both periods of background measurement.

2.8.2. Results

The raw data recorded by the MINN types during their irradiations in the plume simulation setup is represented in Fig. 8.

The inherent background and the contributions to the dose rate indication caused by natural radiation have not been subtracted yet. This form of measurement data would normally be encountered with a typical non-governmental network.

Almost all MINN data enable one visually to conclude if there is a qualitative difference between the background and source measurement, except for the MINN type 10 whose background data and measurement of source 2 are very similar.

Remarkably, the MINN types 13, 16–18 measure visibly larger (other types have similar) dose rates with the source 4 than 3 whereas for the

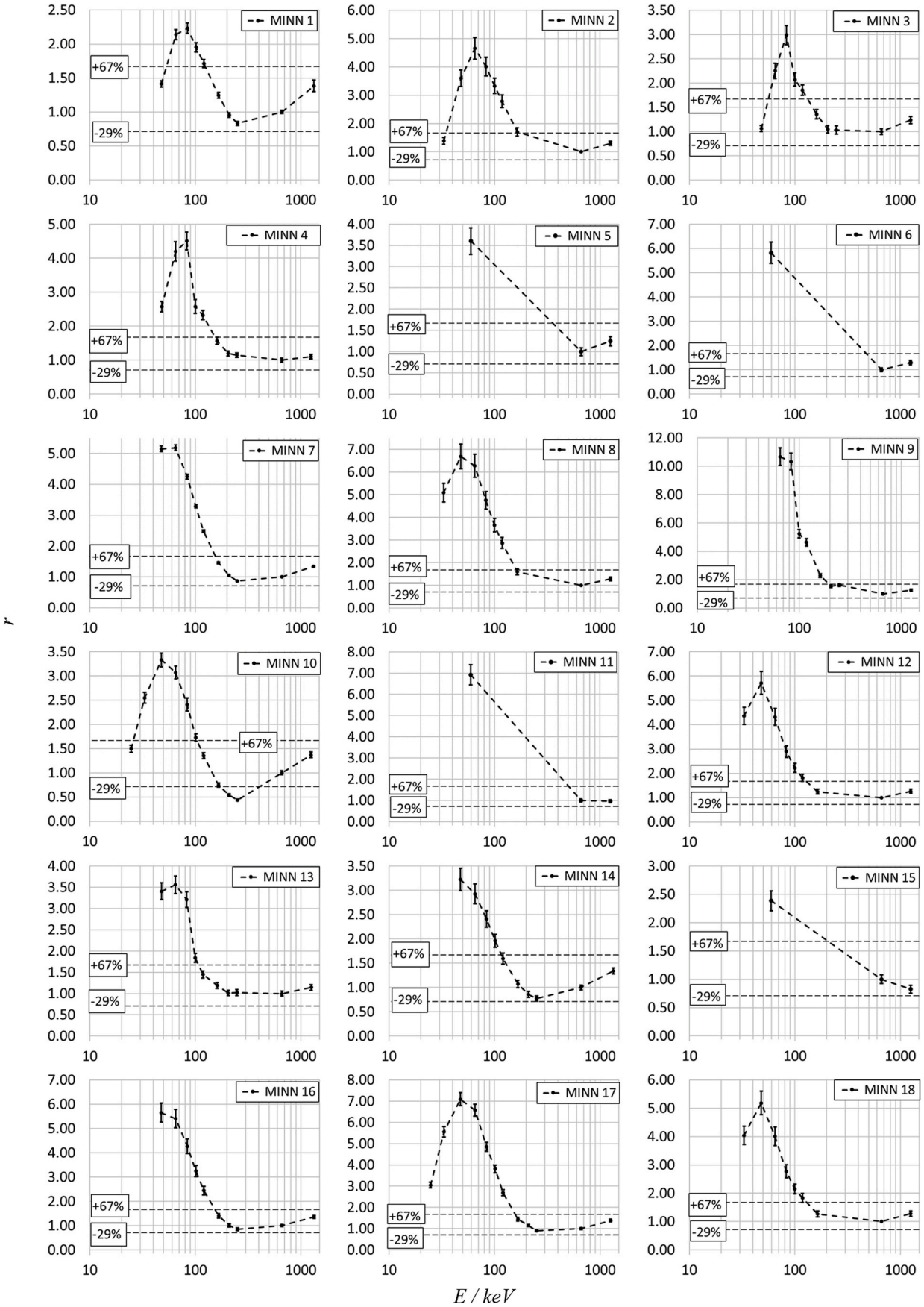

Fig. 6. Energy response of investigated MINN types. The dashed lines between data points serve as the guide to the eye. The dashed straight lines in parallel to x axis indicate the lower and upper acceptable deviation limits defined in IEC 60846–1.

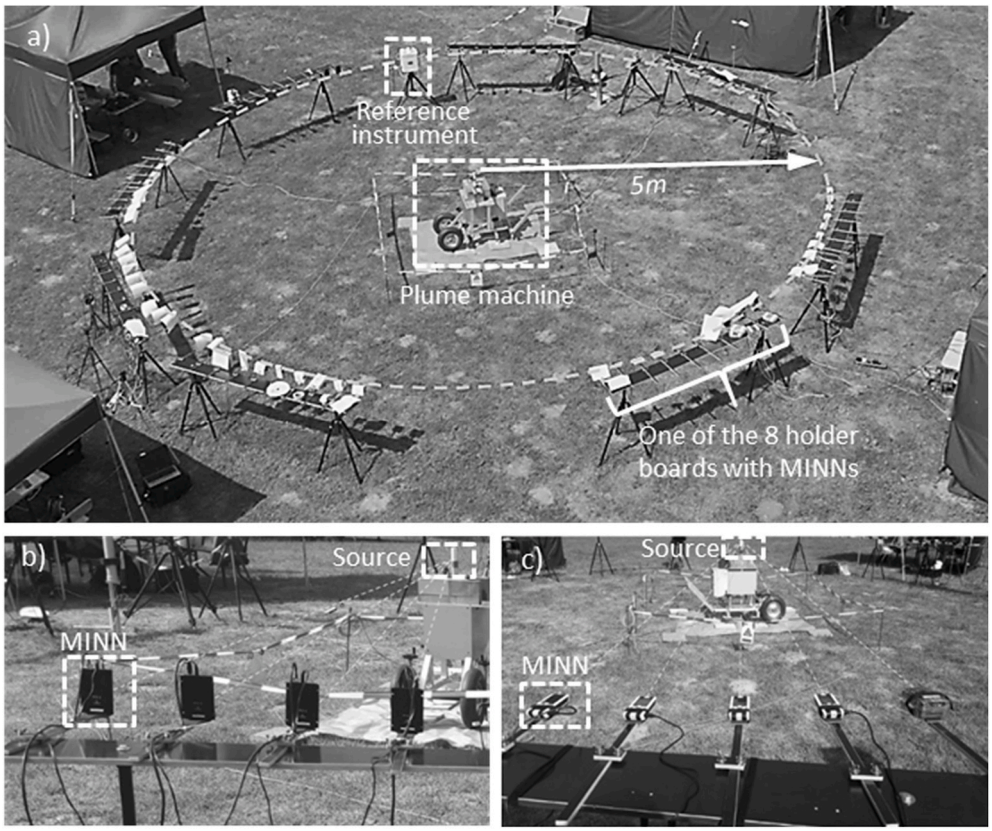

Fig. 7. Plume simulation setup for measurements of small dose rate changes in the environment with natural background radiation. The plume machine in the center of circle surrounded by measurement instruments (a). Vertically (b) and horizontally (c) positioned MINNs.

Table 4
dose rates used during the plume simulation test which are determined by the calibrated reference instrument of the type RS-131.

Nr.	Source	$\dot{H}^{*}(10)_{ref,\,art}$, nSv h^{-1}	$\Delta\dot{H}^{*}(10)_{ref,\,art}$, (k = 2), nSv h^{-1}	timeline
0	BG	75.8	4.6	11:50:27–12:20:29
1	Cs-137	236	14	12:22:26–12:52:27
2	Cs-137	62.0	3.6	12:54:42–13:24:43
3	Cs-137	131.2	7.5	13:25:26–13:55:28
4	Co-60	114	2.9	13:57:32–14:27:33
5	Ra-226	381	14	14:39–15:12
6	Co-60	164	3.9	15:20:08–15:50:10
0	BG	75.8	4.6	15:51:12–16:21:12

$\dot{H}^{*}(10)_{ref,\,art}$ values of those photon fields the opposite is valid. This effect originates in the slightly enhanced sensitivity of the GM sensors to the photons with energies larger than 662 keV (Cs-137) as it was shown above.

The MINNs seem to implement no longer-duration averaging methods on-board beside the acquisition time when storing the data to the memory once per minute. In contrast, for the dose rate displayed on the screen the rolling average method is likely to be applied in some of the MINN types. As a result, the response time to a change of the ambient dose equivalent rate does not exceed the acquisition time for most of the MINN types in this study. It can be seen at the good coincidence of the beginning and the end of dose rate changes measured by the MINNs and by the reference instrument. It was found that the MINN types 8, 10 and 17 are prone to non-critical data loss. The data loss observed for MINN types 5 and 15 during source 6 was due to a power supply fault, not a fault with the MINNs. The response of MINN type 11 during exposure to source 5 was found to be erratic, with the dose rate dropping sharply before recovering over the period of 60 s. This appeared to be consistent with the GM tube intermittently losing power. This was most likely a fault of the USB hub providing power for the four individual MINNs.

In comparison with the absolute values of the reference ambient dose equivalent rate, the MINN types 1 and 4 demonstrate the best performance for the background as well as for the combined background-source measurements. The MINN types 5, 7, 8, 11–14, and 17 show satisfactory measurement results only for the combined background-source measurements and their background readings are slightly enhanced. The MINN types 2, 3, 15 and 16 indications are too high and MINN types 9 and 10 too low compared with the reference values in this test.

The considered raw readings must be corrected for self-effect or inherent background and for overresponse to SCR. Additionally, it should be accounted for different sensitivities of GM sensors to the terrestrial and artificial sources of radiation according to Eq. (1). However, in a real case scenario there is a lack of the reference data and Eq. (5) can be applied, instead.

The final values of $\dot{G}_{type}$ represent the increase of the indication due to an artificial source and are given after subtraction of the MINN background mean value $\dot{G}_{BG}$ from the mean value calculated from the readings taken from one single irradiation period $\dot{G}_{MINN}$. Then, the mean values were averaged within the type. The maximum value of the uncertainties within the set of four MINNs of the same type was selected. This can be justified through the observation that the uncertainties of the same MINN type under identical test conditions in this study are similar. Furthermore, it was assumed that the uncertainty of an individual MINN is representative for the whole type. The results are represented in Fig. 9.

The abscissa of Fig. 9 (a) represents the source number which corresponds to the one of Table 4. Reference values are shown with an

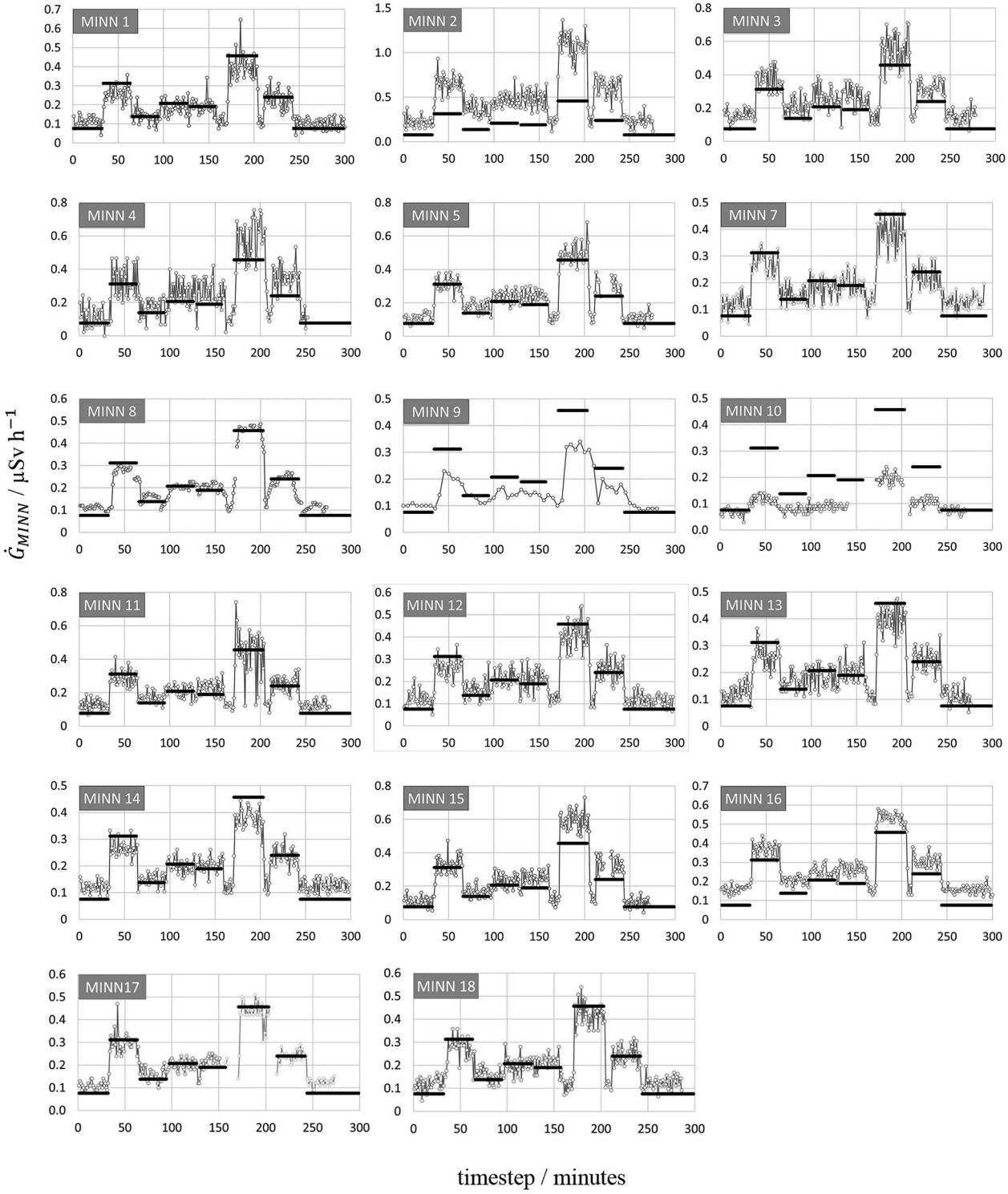

Fig. 8. Raw measurement data from one MINN of each type irradiated at the plume simulation site. The connected points show 1-min averages of the MINN and the solid lines depict combined reference ambient dose equivalent rate values (background and source) corresponding to each irradiation period.

additional solid line over the corresponding MINN type mean values that were evaluated by the irradiation with a source. The dashed lines depict the upper and the lower values of the confidence interval with the coverage factor of 2 belonging to the reference values. On the diagram, the MINN types 1, 7, 9–14, 17 and 18 clearly underestimate the dose rate generated by the artificial sources. The MINN types 2, 8, 11, 16 demonstrate a satisfactory performance at sources 4, 6 (Co-60) and 5 (Ra-226) and underestimate the dose rate at sources 1 and 3 (Cs-137). The MINN types 4 and 15 perform well in the Cs-137 photon fields but demonstrate an overestimation of the dose rate at Co-60 and Ra-226 caused radiation. These results can be explained by poor energy dependence but also by the deviation from linearity at very low dose rate ranges, comparable with natural background. However, most of the calculated values for absolute response are within 30% margin around the reference values, which can be considered satisfactory based on the requirements for energy dependence and linearity given in the relevant

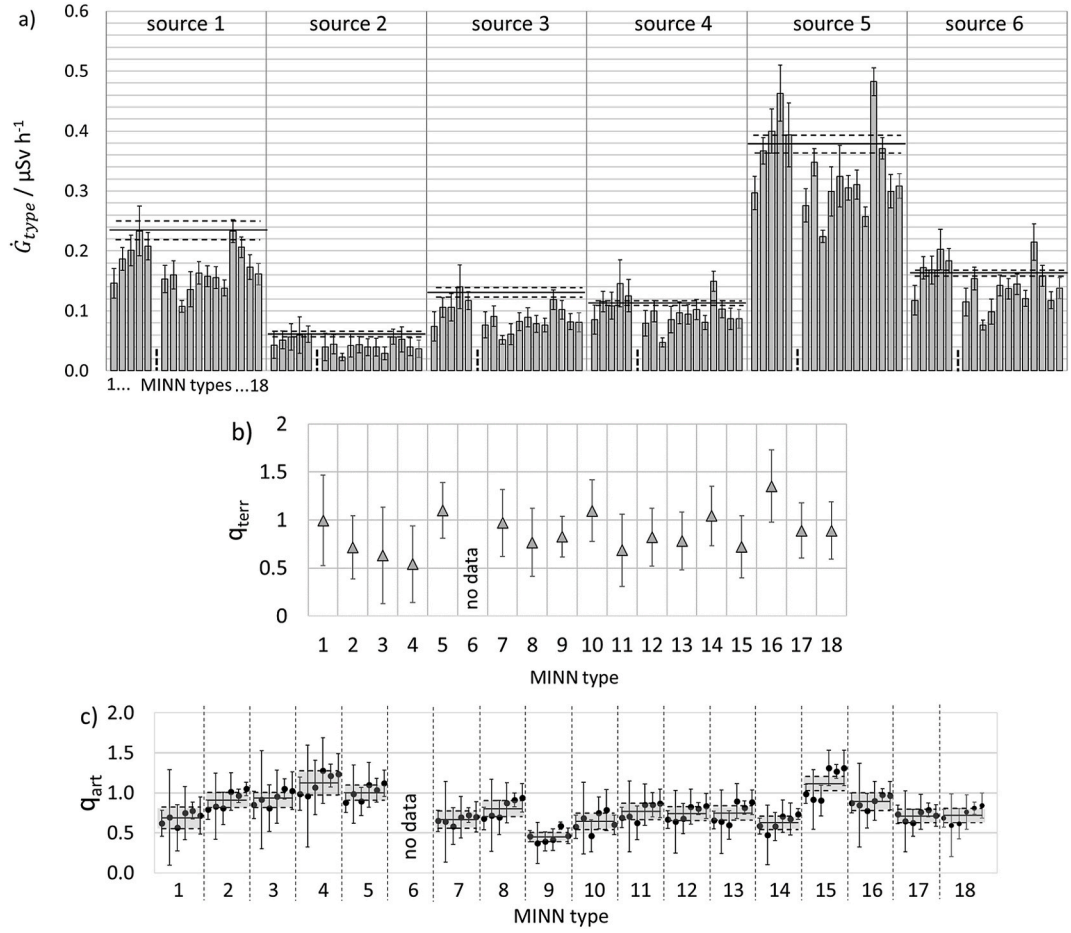

Fig. 9. (a) Absolute dose rate values measured by MINN averaged over four devices of the same type. Solid and dashed lines show the reference values and their uncertainties. Short vertical lines indicate the missing data for the MINN type 6; (b) response of MINN expressed as the averaged measured dose rate in relation to the corresponding reference value calculated with Eq. (1); (c) MINN type sensitivity at the six photon fields generated at the plume simulation site. The six points represent the sensitivity of the corresponding MINN type at photon fields 1 to 6, respectively. Solid and dashed lines depict the average of the six mean values and its uncertainty interval (gray colored) for each MINN type, respectively.

standards (IEC 60846–1).

The diagram in Fig. 9 (b) shows the sensitivity factor of the MINN types to the terrestrial radiation q_{terr} calculated with Eq. (1). Most of the MINN types in the current study have this factor around or close to unity.

Finally, in the diagram of Fig. 9 (c) the MINN type sensitivity factor q_{art} is evaluated for each of the sources used in the plume simulation. Since most of the q_{art} values have their uncertainty intervals overlapping at the investigated dose rates it is reasonable to average the values belonging to the same MINN type for all six constant ambient dose equivalent rate values in this test. As a result, each averaged q_{art} factor has the improved uncertainty interval which still encompasses all points of each MINN type. One exception is the MINN type 9 at the photon field number 5 which demonstrates very low uncertainty at the highest value of ambient dose equivalent rate in this test.

The determination of the characteristic limits - decision threshold and detection limit - for the MINN types was not targeted in this study and is even not useful at this stage. Moreover, the proper calibration of all MINN types in terms of ambient dose rate equivalent is mandatory for the appropriate calculation of these figures. The results would be misleading otherwise. The investigation of these characteristics could be the subject of a separate study or a part of an official calibration procedure.

2.9. Comparison with instruments used in governmental early warning networks

Professional detector systems installed in early warning networks participated in intercomparisons at PTB in the past (Neumaier and Dombrowski, 2014), (Saez Vergara et al., 2007), (Neumaier et al., 2000b), (Wissmann and Sáez Vergara, 2006), (Dombrowski et al., 2009). There are different types of sensors utilized in these instruments among them ionization chambers (IC), Geiger-Mueller sensors (GM) and proportional counters (PC).

Data obtained from detectors used in early warning networks are usually given as 10-min average of ambient dose equivalent rate. Thus, the measurements of a representative MINN of the type 1 during plume simulation ~~in~~ from the current study have been averaged to 10-min values and plotted together with similar data taken by some professional instruments from early warning networks during intercomparisons in the past. In the presented data, the contributions caused by the naturally occurred radiation and the inherent background have been determined and subtracted as the background measurement. It should be noted that the plume simulation test was carried out as part of this intercomparison using identical equipment and parameters (plume simulator, shielding types, distances, sources), however, with some dose rate values different than in the past. Results are plotted in Fig. 10.

In previous intercomparisons with systems from governmental networks, the 001/IC always served as reference instrument and its data

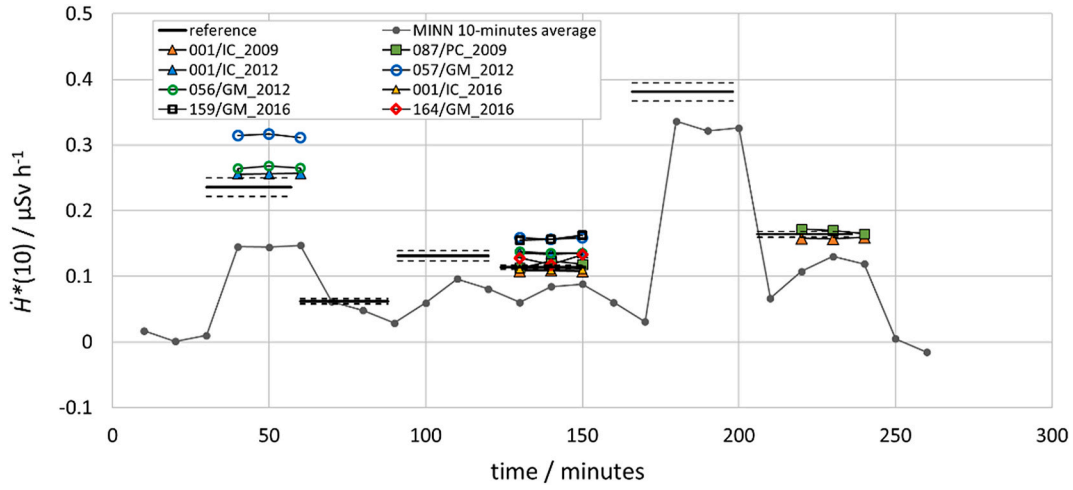

Fig. 10. Comparison of plume simulation data of current MINN intercomparison and of the instruments used in governmental networks taken during previous intercomparisons at PTB in the years 2009, 2012 and 2016.

should be considered as reference values. Their timestep has been adapted to the MINN timestep. The reference values valid for this MINN study are depicted as solid and their confidence intervals as dashed lines.

The shift in the 10-min representation of the MINN data comes from setting the calculation start point to the first 1-min measurement and the result was assigned the last 1-min point. The plot shows a noticeable discrepancy between governmental instruments and the MINN. Detector systems from governmental networks - especially those employing GM sensors - show a slight overestimation of the ambient dose equivalent rate. However, their indication is more stable during an irradiation period. In contrast, the 10-min MINN data shows a significant underestimation of the reference values and greater fluctuation at the lowest investigated ambient dose equivalent rate values.

3. Conclusions

In this comprehensive study of relatively simple, light-weighted and cheap dose rate Measurement Instruments used in Non-governmental dosimetry Networks (MINNs), 68 detectors in total, were tested in four dosimetry laboratories. The two national metrology institutes, PTB and NPL and two designated institutions ENEA and VINCA provided irradiation facilities with dose rate values traceable to primary standards. Using these facilities as well as the unique reference facilities at PTB for dosimetry at low dose rates, the most relevant performance parameters (detector's inherent background, energy dependence and linearity of the response, sensitivity to secondary cosmic radiation, response to small changes of the dose rate, stability of the detector's reading at various climatic conditions) were investigated.

The results of these investigations reveal that the most serious problem of dose rate measurements using these MINNs is their very strong energy dependence, which was found for all tested types. In some cases, an over-response that exceeds the acceptable upper limits as defined in IEC 60846-1 by up to a factor of 6.7 was found. The cause of this problem is the use of non-compensated GM tubes with a bad inherent energy dependence. This problem could in principle be solved by using appropriate energy compensation filters (Kržanović et al., 2019). The latter could only be done by the MINN-manufacturers but certainly not by the laypersons that typically own and operate such simple devices. The results of this intercomparison exercise show that the calibration factors applied by the manufacturers can deviate significantly for some of the systems. Both, the introduction of energy compensation filters and correct (traceable) calibrations by the manufacturers is strongly recommended, but this would probably lead to an increase of the price of such systems, dedicated for citizen science networks.

Concerning the other basic performance parameters: All MINNs showed satisfactory inherent background values of the order of a few tens of nSv·h^{-1}, and most of them also showed a satisfactory linearity of the response for dose rates of up to 100 µSv h^{-1} and above. An over-response to secondary cosmic radiation was found (about 50%), which is typical for GM counters. Finally, in a climate cabinet, the dependence of the dose rate indication of the MINNs under different climate conditions was studied. Concerning their use within the temperature and humidity range specified by the manufacturers (typically −20 °C to +40 °C and a relative humidity between 50% and 95%), with exception of the systems of one manufacturer, all other systems showed stable working and no significant influence of the readings. In contrary, the malfunctioning systems showed no readings at all (0 cpm) and should definitely not be used in the natural environment.

In order to study the sensitivity of the systems to small artificial increases of the dose rate (as caused by a radioactive plume that passes by or by contaminations due to a radioactive fallout), the MINNs were exposed to a natural radiation environment at PTB, superimposed by weak radiation fields, generated by various radioactive sources. All MINN types, except for one, showed a statistically significant increase of the count rates, even for a moderate increase of 60 nSv h^{-1} (i.e. about the same order of magnitude as the natural background radiation at sea level). This means, that MINNs would be able to detect relevant dose rate increases, as typical for accidents with massive release of radioactivity. The MINNs investigated, typically comprise GM tubes featuring small dimensions, which means that longer integrations times are necessary for reasonable statistics, but, on the other hand, lead to a less pronounced angular dependence of the response. Nevertheless, inappropriate location or orientation of the MINNs (e.g. indoors or near to buildings or inside of cars) may significantly influence their dose rate readings.

None of the tested MINN types fully conforms with the relevant dosimetric standards and they all show inferior performance when compared with dedicated dosimeters used by governmental networks. Nevertheless, in case of nuclear or radiological emergency, the possibly large amount of data obtained by non-governmental networks (NRMNs) using MINNs could presumably be used to track radioactive plumes and to detect radioactive contaminations. Both provide extremely relevant information for radiation protection measures of the local authorities, national governments and the European Commission. However, such information based on non-governmental measurements using MINNs should be used with great precautions, considering the possibility of reporting of faked data or of malfunctioning MINNs. In addition, the

NRMNs are sometimes not able to keep the data up to date, due to manual data up-load.

Therefore, comparison with other nearby MINNs and with data from stationary or mobile governmental detector systems will be a prerequisite for an appropriate quality assurance.

Funding

This project (16ENV04 Preparedness) has received funding from the EMPIR programme. The EMPIR initiative is co-financed by the European Union's Horizon 2020 research and innovation programme and the participating states within EURAMET.

Declaration of competing interest

The authors declare that they have no known competing financial interests or personal relationships that could have appeared to influence the work reported in this paper.

Acknowledgements

The authors would like to thank Jörg Kretzer, Roland Zwiener, Karsten Kahnt, Christian Fuhg, Patrik Kramer, Maksym Luchkov, Phil Brüggemann, Jürgen Roth, Bjoern Pullner, Marcel Lebbing for their support during the preparations, while conducting the tests at PTB and Dr. Oliver Hupe, Dr. Hayo Zutz, Dr. Harald Dombrowski and Dr. Konstantins Bogucarskis for valuable discussions.

References

Basuki, T., Bekelesi, W.C., Tsujimoto, M., Nakashima, S., 2020. Investigation of radiocesium Migration from Land to Waterbody using radiocesium Distribution and Soil to sediment ratio: a Case of the steep slope catchment Area of ogi reservoir, kawauchi village, Fukushima. Radiation Safety Management 19, 23–34.

Bonnett, P.J.P., 1990. A review of the erosional behaviour of radionuclides in selected drainage basins. J. Environ. Radioact. 11, 251–266.

Bossew, P., Cinelli, G., Hernández-Ceballos, M.A., Cernohlavek, N., Gruber, V., Dehandschutter, B., Bleher, M., Hellmann, I., Weiler, F., Tollefsen, T., Tognoli, P.V., De Cort, M., 2017. Estimating the terrestrial gamma dose rate by decomposition of the ambient dose equivalent rate. J. Environ. Radioact. 166, 296–308.

Brown, A., Franken, P., Bonner, S., Dolezal, N., Moross, J., Safecast, 2016. Successful citizen-science for radiation measurement and communication after Fukushima. J. Radiol. Prot. 36, S82.

Bunzl, K., Schimmack, W., Kreutzer, K., Schierl, R., 1989. *Interception and retention of Chernobyl-derived ^{134}Cs, ^{137}Cs and ^{106}Ru in a spruce stand.* Sci. Total Environ. 78, 77–87.

Chartin, C., Evrard, O., Laceby, J.P., Onda, Y., Ottlé, C., Lefèvre, I., Cerdan, O., 2017. The impact of typhoons on sediment connectivity: lessons learnt from contaminated coastal catchments of the Fukushima Prefecture (Japan). Earth Surf. Process. Landforms 42, 306–317.

Coletti, M., Hultquist, C., Kennedy, W.G., Cervone, G., 2017. Validating safecast data by comparisons to a U. S. Department of energy Fukushima prefecture aerial survey. J. Environ. Radioact. 171.

Corson, D.R., Wilson, R.R., 1962. Particle and quantum counters. Rev. Sci. Instrum. 19, 207–233.

Dombrowski, H., Neumaier, S., Thompson, I.M.G., Wissmann, F., 2009. EURADOS intercomparison 2006 to harmonize European early warning dosimetry systems. Radiat. Protect. Dosim. 135, 1.

Gonze, M.A., Calmon, P., 2017. Meta-analysis of radiocesium contamination data in Japanese forest trees over the period 2011–2013. Sci. Total Environ. 601/602, 301–316.

http://www.preparedness-empir.eu/. (Accessed 1 August 2020).

Hultquist, C., Cervone, G., 2018. Comparison of simulated radioactive atmospheric releases to citizen science observations for the Fukushima nuclear accident. Atmos. Environ. 198, 478–488.

International Electrotechnical Commission, 2009. Radiation Protection Instrumentation - *Ambient And/or Directional Dose Equivalent (Rate) Meters And/or Monitors for Beta, X and Gamma Radiation - Part 1: Portable Workplace And Environmental Meters And Monitors.* IEC 60846-1.

International Organization for Standardization, 1995. "*Guide To the Expression of Uncertainty in Measurement*", Report ISO/DGuide 99998. ISO), Geneva.

Iso 4037-1:2019, 2019. Radiological Protection — X and Gamma Reference Radiation for Calibrating Dosemeters and Doserate Meters and for Determining Their Response as a Function of Photon Energy — Part 1: Radiation Characteristics and Production Methods.

Iurlaro, G., et al., 2018a. Monitoring of Ionising Radiation by Non-governmental Networks in the Framework of the Empir - 16env04 "Preparedness" Project, Book of Abstract 4th NERIS Workshop, "*Adapting Nuclear and Radiological Emergency Preparedness, Response and Recovery to a Changing World*", p. 54.

Iurlaro, G., et al., 2018b. "Environmental Measurements of Radioactivity and Radiation Protection Quantity Available in Non-governmental Network Web Sites", Book of Abstract 3rd European Radiation Protection Week 2018, pp. 110–111. https://erpw2018.com/wp-content/uploads/2018/09/ERPW-abstracts-book_web_pages.pdf. (Accessed 1 August 2020).

Komissarov, M.A., Ogura, S., 2017. Distribution and migration of radiocesium in sloping landscapes three years after the Fukushima-1 nuclear accident. Eurasian Soil Sci. 50, 861–871.

Kržanović, N., Stanković, K., Živanović, M., Đaletić, M., Ciraj-Bjelac, O., 2019. Development and testing of a low cost radiation protection instrument based on an energy compensated Geiger-Müller tube. Radiat. Phys. Chem. 164.

Livens, F.R., Fowler, D., Horrill, A.D., 1992. *Wet and dry deposition of ^{131}I, ^{134}Cs, and ^{137}Cs at an upland site in northern England.* J. Environ. Radioact. 16, 243–254.

Neumaier, S., Dombrowski, H., 2014. EURADOS Intercomparisons and the harmonization of environmental radiation monitoring. Radiat. Protect. Dosim. 160 (No. 4), 297–305.

Neumaier, S., Arnold, D., Boehm, J., Funck, E., 2000a. The PTB underground laboratory for dosimetry and spectrometry. Appl. Radiat. Isot. 53, 173.

Neumaier, S., Funck, E., Saez-Vergara, J.C., 2000b. The PTB contribution to the 1999 EURADOS intercomparison of national early warning systems. Radiat. Protect. Dosim. 92, 101–108.

Neumaier, S., et al., 2019. *Metrology for the mobile detection of ionising radiation following a nuclear or radiological incident* – "Preparedness". Arh. Hig. Rada. Toksikol. 70, 62–68, 2019.

Poreba, G., Bluszcz, A., Oenieszko, Z., 2003. *Concentration and vertical distribution of ^{137}Cs in agricultural and undisturbed soils from Chechlo and Czarnocin areas.* Geochronometria 22, 67–72.

ICRU report 92 - *radiation Monitoring for Protection of the Public after major Releases of Radionuclides to the environment.* J. ICRU 15 (1–2), 2015, 92–94. Report 92, 2015.

Röttger, A., Kessler, P., 2019. Uncertainties and characteristic limits of counting and spectrometric dosimetry systems. J. Environ. Radioact. 205–206. S. 48-54.

Saez Vergara, J.C., et al., 2007. The second EURADOS intercomparison of national network systems used to provide early warning of a nuclear accident. Radiat. Protect. Dosim. 123, 190–208.

Sangiorgi, M., Hernández-Ceballos, M.A., Jackson, K., Cinelli, G., Bogucarskis, K., De Felice, L., Patrascu, A., De Cort, M., 2020. The European radiological data Exchange platform (EURDEP): 25 years of monitoring data exchange. Earth Syst. Sci. Data 12, 109–118. https://doi.org/10.5194/essd-12-109-2020.

Sperandio, L., Iurlaro, G., Kessler, P., Marganiec, J., Bogucarskis, K., De Cort, M., 2018. *Indagine sulle Reti non governative di monitoraggio delle radiazioni ionizzanti nell'ambito del progetto EMIPR-16ENV04 "Preparedness"*", XXXVII Congresso Nazionale di Radioprotezione, ISBN 9788888648460, pp. 270–280. https://www.airp-asso.it/wp-content/uploads/convegni/2018_Bergamo/ATTI.pdf.

16ENV04 Preparedness, Publishable Summary for 16ENV04 "Preparedness", *Metrology for Mobile Detection of Ionizing Radiation Following a Nuclear or Radiological Incident*, 2018.

von Droste, G.F., 1937. Z. Phys. 104, 474.

Wallbrink, P.J., Murray, A.S., 1993. Use of fallout radionuclides as indicators of erosion processes. Hydrol. Process. 7, 297–304.

Wissmann, F., 2006. Variations observed in environmental radiation at ground level. Radiat. Protect. Dosim. 118 (1), 3–10.

Wissmann, F., Sáez Vergara, J.C., 2006. Dosimetry of environmental radiation—a report on the achievements of WG 3. Radiat. Protect. Dosim. 118 2, 167–175.

Wissmann, F., Dangendorf, V., Schrewe, U., 2005. Radiation exposure at ground level by secondary cosmic radiation. Radiat. Meas. 39, 95–104.

Yoshimura, K., Onda, Y., Wakahara, T., 2016. *Time Dependence of the ^{137}Cs Concentration in particles Discharged from rice Paddies to freshwater Bodies after the Fukushima Daiichi NPP accident.* Environ. Sci. Technol. 50, 4186–4193.

Yukawa, Sakata, 1937. Sci. Pap. Inst. Phys. Chem. Res. 31, 187.